NANO LETTERS

pubs.acs.org/NanoLett

Letter

Revealing and Quantifying Carbon Corrosion in Aqueous Manganese-Based Batteries

Ajay Ravi, Ge Zhang, John Holoubek, Yuqi Li, Hongchang Hao, Angela Cai, Sanzeeda Baig Shuchi, Guangxia Feng, Jingyi Han, Jinlei Li, Stacey F. Bent, Xueli Zheng,* and Yi Cui*

Cite This: *Nano Lett.* 2025, 25, 10834−10839

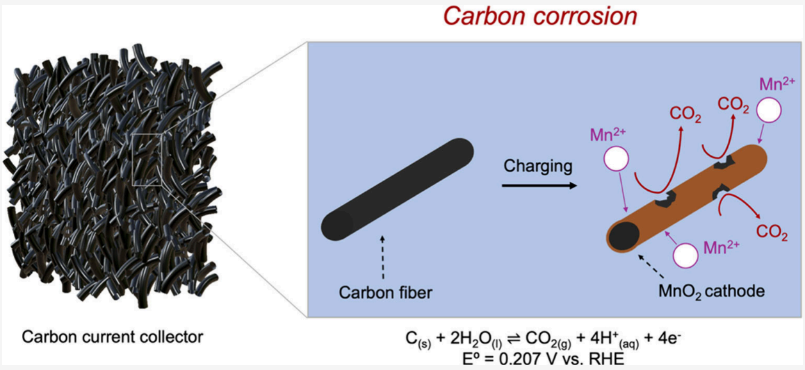

ABSTRACT: The MnO_2/Mn^{2+} cathode chemistry represents a promising avenue for high-energy-density and low-cost aqueous batteries. However, its practical application for grid-scale storage is limited by insufficient cycling stability. Extensive reports have highlighted the poor reversibility of MnO_2 deposition and stripping. Here, we reveal an overlooked source of capacity loss under typical operating conditions: corrosion of the carbon current collector. Using gas chromatography, we show that carbon corrosion can account for up to ∼25% of initial capacity losses and can cause thickness losses approaching 200 nm in the first cycle. Corrosion-induced thickness losses are largest under acidic and near-neutral conditions. Corroborating our corrosion measurements, X-ray photoelectron spectroscopy and scanning electron microscopy results indicate the formation of surface oxygen species and carbon fiber degradation after cycling. Our work provides a quantitative understanding of carbon corrosion in aqueous batteries that can inform strategies for extending their cycle life.

KEYWORDS: *aqueous batteries, carbon corrosion, MnO_2 cathode, grid-scale storage, gas chromatography*

The intermittency of renewable energy sources, such as solar and wind, necessitates the development of sustainable energy storage systems.[1,2] The efficacy of stationary storage can be evaluated primarily on the basis of (1) levelized energy cost, expressed as \$/(kWh·cycle), and (2) safety.[3] Given the supply chain limitations of lithium and the flammability concerns with organic liquid electrolytes, it is worthwhile to consider the use of earth-abundant elements and aqueous electrolytes for grid-scale energy storage.[3,4] One promising cathode for aqueous cells is the MnO_2/Mn^{2+} chemistry, which operates via deposition−dissolution reactions between soluble Mn^{2+} and solid MnO_2 deposited on a carbon current collector.[5−9] Given the high redox potential of Mn^{2+}/MnO_2 (1.23 V vs RHE) and the high theoretical capacity of MnO_2 (616 mAh/g for two-electron transfer), this environmentally friendly cathode can provide aqueous batteries with high energy density.[8]

Despite its great potential, the Coulombic efficiency (CE) and cycling stability of the MnO_2 cathode are not sufficient for its application in practical aqueous batteries. A number of studies have focused on the sources of irreversibility associated with the Mn^{2+}/MnO_2 dissolution−deposition reaction.[9−12] For example, researchers have shown that the reversibility of Mn^{2+}/MnO_2 is limited by the poor conductivity of the typical deposition product ε-MnO_2, the competitive oxygen evolution reaction, and the accumulation of "dead Mn."[9] Considerable efforts have been devoted to developing strategies to improve the reversibility of MnO_2 deposition and stripping.[8,10,13−16]

However, the loss of CE from current collector corrosion remains overlooked in aqueous manganese-based batteries. Carbon felt is widely used as the cathode current collector,

Received: April 13, 2025
Revised: June 19, 2025
Accepted: June 23, 2025
Published: June 27, 2025

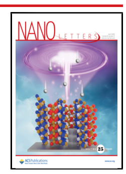

https://doi.org/10.1021/acs.nanolett.5c02166
Nano Lett. 2025, 25, 10834−10839

owing to (1) its low cost; (2) its high surface area; (3) its greater resistance to electrochemical oxidation compared to other inexpensive current collectors (e.g., aluminum); and (4) its relatively low activity for the oxygen evolution reaction. Yet, carbon is also prone to corrosion in aqueous batteries, and the associated CE losses represent a crucial factor that can limit the overall longevity of the battery. While carbon corrosion has not been investigated in aqueous manganese-based batteries, this problem has been explored in catalysis.[17−21] From catalysis literature, it is known that corrosion of carbon-based supports is most pronounced at high operating potentials and in acidic environments.[17,18] Carbon corrosion has been observed to cause losses in the electrochemically active surface area and the electrical conductivity of the support structure.[18] The degradation mechanism of carbon supports is generally attributed to the following electrochemical reaction:

$$C_{(s)} + 2H_2O_{(l)} \rightleftharpoons CO_{2(g)} + 4H^+_{(aq)} + 4e^- \quad E^\circ = 0.207 \text{ V vs RHE} \tag{1}$$

We anticipate that this corrosion reaction is also relevant to the carbon current collector for the MnO_2 cathode. While the thermodynamic potential of carbon corrosion is relatively low, the kinetics of carbon corrosion are sluggish until >1 V vs RHE.[21,22] It should be emphasized that MnO_2 deposition (E° = 1.23 V vs RHE) occurs within this regime where corrosion kinetics are non-negligible. In this work, we show that the carbon current collector can be oxidized to CO_2 under typical operating conditions (Figure 1). As illustrated in Figure 1, the carbon corrosion reaction takes place primarily during charging concurrently with the electrodeposition of MnO_2. We demonstrate this phenomenon by using gas chromatography (GC) to measure the CO_2 evolved after charging, which enables us to quantify corrosion-induced CE losses as well as thickness and mass losses. In the Zn−MnO_2 battery,[6,23] we find that carbon corrosion can account for up to ∼25% of first-cycle CE losses and can induce thickness losses and mass losses of ∼200 nm and ∼2 $\mu g/cm^2$, respectively. In conjunction with our GC measurements, we examine the structural and chemical changes of the current collector using scanning electron microscopy (SEM) and X-ray photoelectron spectroscopy (XPS). Through this work, we hope to raise awareness of an overlooked corrosion process in aqueous manganese-based batteries and aqueous batteries more broadly.

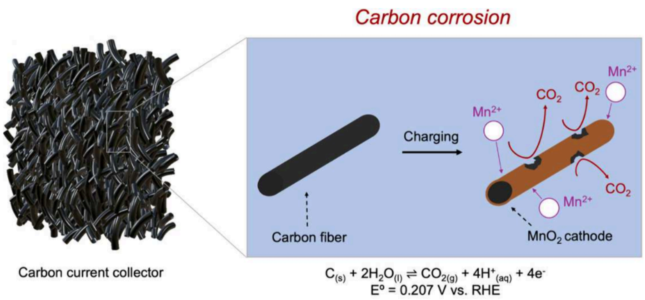

Figure 1. Schematic illustration of carbon corrosion showing the oxidation of the current collector concurrently with MnO_2 deposition during charging.

Figure 2a shows the first-cycle voltage profile of the Zn−MnO_2 battery, charged at a typical voltage of 2.2 V up to 1 mAh/cm^2 and discharged at a moderate rate of 4C in a representative electrolyte (0.1 M H_2SO_4 + 1 M $ZnSO_4$ + 1 M $MnSO_4$, pH: 1.1). It can be seen that the first-cycle CE, averaged over four cells, is 96.64% (Figure S1), meaning that the total first-cycle CE loss (ΔCE) is −3.36%. Here, we set out to determine the proportion of this ΔCE that is attributable to carbon corrosion. We do so by first measuring the CO_2 evolved upon charging using GC and then backcalculating the associated capacity loss using Reaction (1). As displayed in Figure 2b and Figure S2, the Zn-MnO_2 battery is assembled within a gastight vial, with Zn foil as the anode and carbon felt as the cathode current collector. The battery is then charged at 2.2 V up to a fixed capacity. After charging, the gas in the headspace of the vial is extracted, and the amount of CO_2 is measured using GC (Figure 2b).

With this procedure, we measure the CO_2 evolved for MnO_2 deposition with nominal areal capacities of 0.5, 1, and 6 mAh/cm^2 (Figure 2c). We find evidence of carbon corrosion at all capacities, and we also see that the CO_2 evolved increases nonlinearly with capacity. When the capacity is doubled from 0.5 to 1 mAh/cm^2, the moles of CO_2 evolved increase by a factor of ∼4. However, from 1 to 6 mAh/cm^2, the CO_2 evolved shows no significant increase, as reflected by the overlapping error bars. In other words, it appears that carbon corrosion slows at higher areal capacities. We attribute this observation to the fact that the MnO_2 deposition during charging can partially protect the carbon current collector from corrosion. Charging up to higher capacities can yield greater coverage of the carbon by MnO_2, resulting in a slower rate of increase in the measured CO_2.

From the moles of CO_2, we calculate the corresponding ΔCE attributable to carbon corrosion at each of the three areal capacities (Figure 2d). We find that the ΔCE is the largest at 1 mAh/cm^2, equaling −0.97%. Comparing this calculated value to the measured total ΔCE (−3.36%), we conclude that carbon corrosion can account for over 25% of the first-cycle CE losses (Figure 2e). Besides the ΔCE, we calculate the mass loss and thickness loss of the carbon current collector for varied capacities, as shown in Figure 2f. The average thickness loss from carbon corrosion can reach nearly 200 nm at 6 mAh/cm^2, and the average mass loss approaches 2 $\mu g/cm^2$.

As noted earlier, these corrosion measurements for varying areal capacity are all obtained in acidic condition. Electrolytes with a pH of ∼1 or lower are most commonly used for aqueous Mn-based batteries; greater acidity can deliver a shorter charge time and a higher discharge potential.[5,24] However, the Zn anode exhibits a better electrochemical performance in less acidic environments. It is worthwhile to examine whether and how changes to the electrolyte pH can affect the corrosion behavior of the carbon current collector.

With this question in mind, we additionally measure the CO_2 evolved after charging at 2.2 V up to 1 mAh/cm^2 in a basic electrolyte (4 M KOH, pH: 14.6) and a near-neutral electrolyte (1 M $Zn(CH_3COO)_2$ + 0.4 M $Mn(CH_3COO)_2$, pH: 6.0).[16,24] Measuring carbon corrosion in the basic condition can be challenging, as CO_2 dissolution will occur as follows: $2OH^- + CO_2 \rightleftharpoons CO_3^{2-} + H_2O$.[17] This issue can be circumvented by acidifying the electrolyte after charging to release dissolved CO_2.[25] Based on a Bjerrum plot, acidifying to a pH of less than 4 is sufficient to shift the CO_2/CO_3^{2-} equilibrium essentially entirely toward CO_2.[17,25] After completing the postcharging acidification, we find that the basic condition is considerably less corrosive to the carbon felt than the acidic condition (Figure 3a). Our observation is

https://doi.org/10.1021/acs.nanolett.5c02166
Nano Lett. 2025, 25, 10834−10839

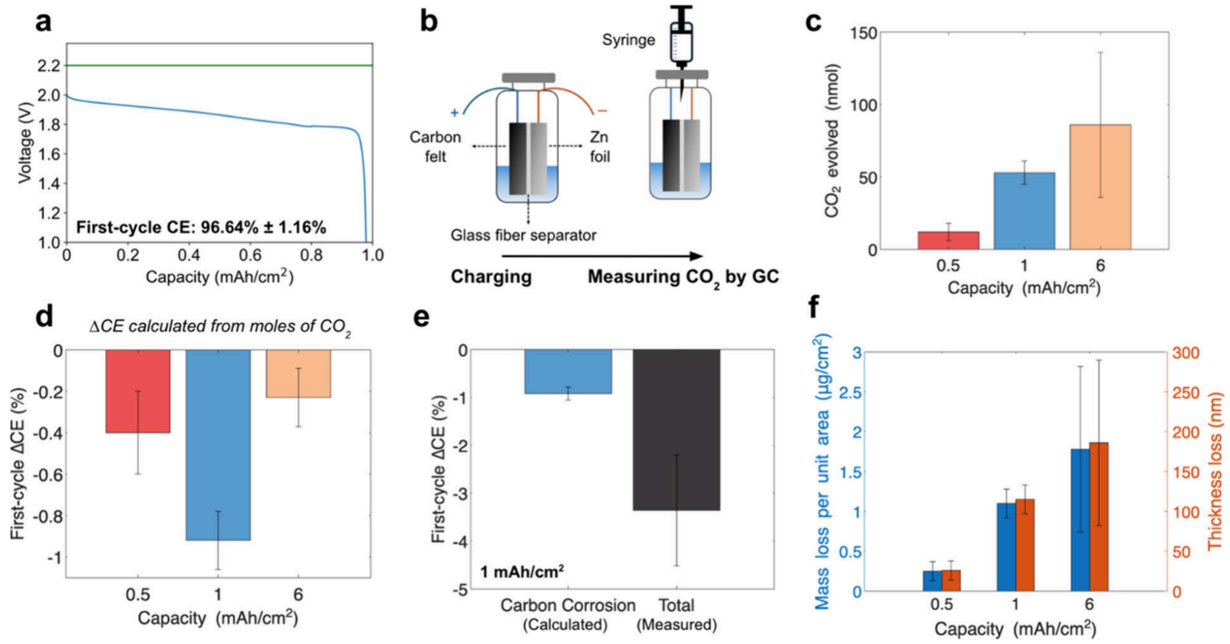

Figure 2. Quantifying carbon corrosion in the Zn−MnO_2 battery. (a) Representative first-cycle voltage profile of the Zn−MnO_2 battery. (b) Schematic illustration of the experimental setup for quantifying carbon corrosion. (c) CO_2 evolution measurements and (d) corresponding first-cycle ΔCE values calculated from the moles of CO_2 for areal capacities of 0.5, 1, and 6 mAh/cm^2. (e) Comparison of ΔCE attributable to carbon corrosion and total ΔCE in the 1st cycle (for a charging capacity of 1 mAh/cm^2). (f) Calculated mass loss per unit geometric area and thickness loss for varied areal capacities. Each value reported from (c)-(f) is determined from an average of at least 3 replicate cells, and error bars represent one standard deviation.

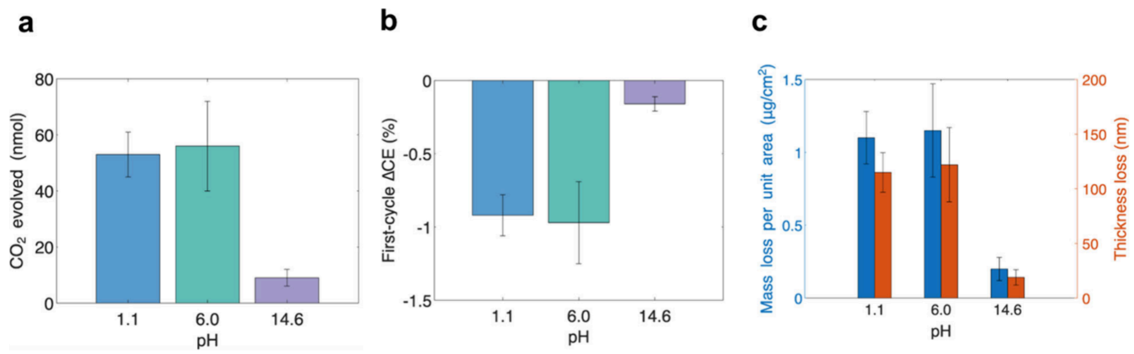

Figure 3. Quantifying carbon corrosion for varied electrolyte pH. (a) CO_2 evolution measurements, (b) calculated corrosion-induced ΔCE, and (c) calculated mass loss per unit geometric area and thickness loss under acidic, basic, and near-neutral conditions. Each value reported from (a)-(c) is determined from an average of 3 replicate cells, and error bars represent one standard deviation.

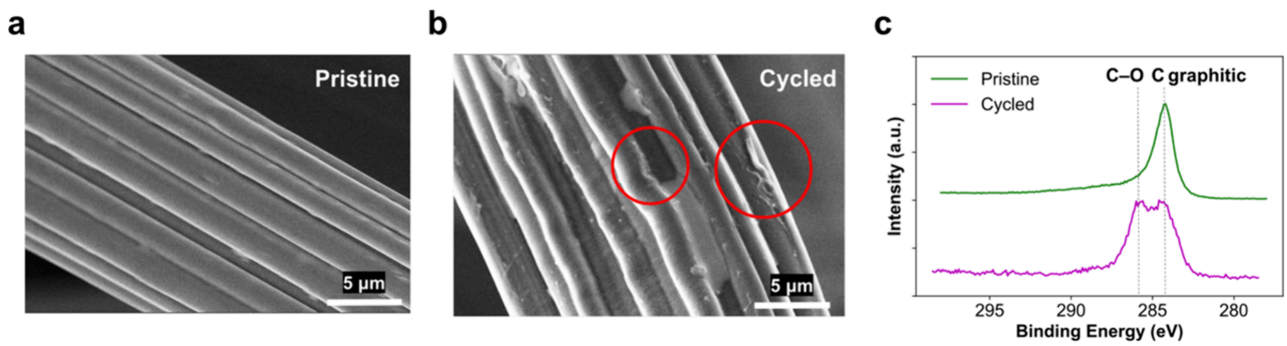

Figure 4. Morphological and chemical changes of the carbon current collector after cycling. SEM images of (a) pristine carbon felt and (b) carbon felt after a potential hold of 2.2 V for 1.5 h in 0.1 M H_2SO_4 + 1 M $ZnSO_4$. (c) XPS C 1s high-resolution spectra for pristine carbon felt and cycled carbon felt (after 100 cycles in the Zn−MnO_2 battery).

consistent with electrocatalysis literature that has reported greater corrosion of carbon supports in acidic conditions than in basic conditions.[17] From a thermodynamics perspective, this result may appear counterintuitive, as increased pH would be expected to correspond to an increased equilibrium concentration of CO_2 (Reaction (1)). However, the kinetics of carbon corrosion are known to be faster in acidic environments, which can result in greater corrosion.[17]

Moving from the basic electrolyte to the near-neutral electrolyte, we notice that the CO_2 evolved is substantially larger and comparable to that in the acidic condition (Figure 3a). The corresponding ΔCE, mass loss, and thickness loss all show the same trend with the acidic and near-neutral conditions giving the greatest corrosion (Figure 3b,c). Whereas the basic condition gives a ΔCE of less than −0.2%, the acidic and near-neutral conditions give a ΔCE of exceeding −0.9%. Similarly, the latter two conditions yield thickness losses above 100 nm, while the basic condition yields a thickness loss below 30 nm.

To complement our quantitative measurements of carbon corrosion, we qualitatively examine the morphological and chemical changes of the carbon current collector. Recognizing that the acidic condition is corrosive to the current collector and most relevant to aqueous Mn-based batteries, we performed SEM and XPS on the carbon felt in this condition. Note that for our SEM experiment, we did not include $MnSO_4$ in our electrolyte; when this salt was included, significant residual MnO_2 was observed after cycling, which rendered it difficult to identify microstructural changes of the carbon felt (Figure S3). After a potential hold of the carbon felt at 2.2 V (vs Zn/Zn^{2+}), we observe degradation of the carbon fiber, which serves as visual evidence of mass loss (Figure 4a,b).[26] To analyze changes in the surface chemical composition, we obtain the XPS C 1s spectrum for the carbon felt after 100 cycles in the $Zn-MnO_2$ battery. As shown in Figure 4c, a peak corresponding to carbon bonded to oxygen (C−O) appears after cycling, which suggests the emergence of surface oxygen functional groups in agreement with previous reports of the intermediate species in the mechanism of carbon corrosion.[27,28]

We emphasize that the observed corrosion of the carbon current collector can limit the cycle life of the aqueous battery. It is reported that carbon corrosion leads to increased charge transfer resistance.[29,30] This effect may exacerbate the already sluggish kinetics of MnO_2 deposition, resulting in an overpotential penalty that yields reduced energy efficiency over long-term cycling. The corrosion-induced losses in electrical conductivity and electrochemically active surface area may also contribute to the aggregation of 'dead MnO_2.'

In summary, using GC, we demonstrate significant carbon corrosion under typical operating conditions of the aqueous manganese-based battery. We find that corrosion is most pronounced under acidic as well as near-neutral conditions and that thickness losses can reach 200 nm. In line with the GC measurements, SEM and XPS results reveal the degradation of the carbon fiber and the formation of surface oxygen species upon cycling. The fundamental understanding of carbon corrosion provided by our report can be applied to improve the reversibility of the MnO_2 cathode. It is also noteworthy that our work represents the first study to quantify CE losses and thickness losses arising from carbon corrosion in an aqueous battery. We propose that our quantitative approach can be extended to study corrosion in other aqueous systems employing carbon-based current collectors.

■ ASSOCIATED CONTENT

Supporting Information

The Supporting Information is available free of charge at https://pubs.acs.org/doi/10.1021/acs.nanolett.5c02166.

Details on the experimental procedures; calculation of moles of CO_2, mass loss, thickness loss, and ΔCE; replicate measurements of first-cycle CE; illustration of the vial battery setup; and additional SEM images (PDF)

■ AUTHOR INFORMATION

Corresponding Authors

Xueli Zheng − *Department of Materials Science and Engineering, Stanford University, Stanford, California 94305, United States; Stanford Institute for Materials and Energy Sciences, SLAC National Accelerator Laboratory, Menlo Park, California 94025, United States;* orcid.org/0000-0002-6800-2649; Email: xuelizh8@stanford.edu

Yi Cui − *Department of Materials Science and Engineering and Department of Energy Science and Engineering, Stanford University, Stanford, California 94305, United States; Stanford Institute for Materials and Energy Sciences, SLAC National Accelerator Laboratory, Menlo Park, California 94025, United States;* orcid.org/0000-0002-6103-6352; Email: yicui@stanford.edu

Authors

Ajay Ravi − *Department of Materials Science and Engineering, Stanford University, Stanford, California 94305, United States;* orcid.org/0009-0003-6648-1206

Ge Zhang − *Department of Materials Science and Engineering, Stanford University, Stanford, California 94305, United States*

John Holoubek − *Department of Materials Science and Engineering, Stanford University, Stanford, California 94305, United States;* orcid.org/0000-0003-0015-4512

Yuqi Li − *Department of Materials Science and Engineering, Stanford University, Stanford, California 94305, United States;* orcid.org/0000-0003-1501-1549

Hongchang Hao − *Stanford Institute for Materials and Energy Sciences, SLAC National Accelerator Laboratory, Menlo Park, California 94025, United States*

Angela Cai − *Department of Materials Science and Engineering, Stanford University, Stanford, California 94305, United States*

Sanzeeda Baig Shuchi − *Department of Chemical Engineering, Stanford University, Stanford, California 94305, United States*

Guangxia Feng − *Department of Materials Science and Engineering, Stanford University, Stanford, California 94305, United States*

Jingyi Han − *Department of Chemical Engineering, Stanford University, Stanford, California 94305, United States*

Jinlei Li − *Department of Materials Science and Engineering, Stanford University, Stanford, California 94305, United States*

Stacey F. Bent − *Department of Chemical Engineering and Department of Energy Science and Engineering, Stanford University, Stanford, California 94305, United States;* orcid.org/0000-0002-1084-5336

Complete contact information is available at: https://pubs.acs.org/10.1021/acs.nanolett.5c02166

Author Contributions

A.R., X.Z., and Y.C. conceived the idea and designed the experiments. A.R. performed all experiments with technical help from G.Z., Jo.H., Y.L., H.H., A.C., S.B.S., G.F., Ji.H., and J.L. Y.C. and X.Z. supervised the overall study. A.R. wrote the first draft of the manuscript and revised it based on input from Y.C., S.F.B., and X.Z. All authors reviewed the manuscript and provided comments.

Notes

The authors declare no competing financial interest.

■ ACKNOWLEDGMENTS

This work is inspired by the Aqueous Battery Consortium, an energy innovation hub under the US Department of Energy, Office of Basic Energy Sciences, Division of Materials Science and Engineering. A.R. acknowledges support from the National Science Foundation Graduate Research Fellowship (DGE-2146755). S.B.S. acknowledges support from TomKat Center Graduate Fellowship for Translational Research and Link Foundation Energy Fellowship. The authors also acknowledge the financial support provided by the US Department of Energy, Basic Energy Sciences, Materials Sciences and Engineering Division, under contract DE-AC0276SF00515. Part of this work was performed at the Stanford Nano Shared Facilities (SNSF) RRID:SCR_023230, supported by the National Science Foundation under award ECCS-2026822.

■ REFERENCES

(1) Rugolo, J.; Aziz, M. J. Electricity storage for intermittent renewable sources. *Energy Environ. Sci.* **2012**, *5* (5), 7151−7160.

(2) Perry, M. L.; Rodby, K. E.; Brushett, F. R. Untapped potential: the need and opportunity for high-voltage aqueous redox flow batteries. *ACS Energy Lett.* **2022**, *7* (2), 659−667.

(3) Wu, X.; Markir, A.; Xu, Y.; Zhang, C.; Leonard, D. P.; Shin, W.; Ji, X. A rechargeable battery with an iron metal anode. *Adv. Funct. Mater.* **2019**, *29* (20), No. 1900911.

(4) Liang, Y.; Yao, Y. Designing modern aqueous batteries. *Nat. Rev. Mater.* **2023**, *8* (2), 109−122.

(5) Chen, W.; Li, G.; Pei, A.; Li, Y.; Liao, L.; Wang, H.; Wan, J.; Liang, Z.; Chen, G.; Zhang, H.; Wang, J.; Cui, Y. A manganese−hydrogen battery with potential for grid-scale energy storage. *Nat. Energy* **2018**, *3* (5), 428−435.

(6) Li, G.; Chen, W.; Zhang, H.; Gong, Y.; Shi, F.; Wang, J.; Zhang, R.; Chen, G.; Jin, Y.; Wu, T.; Tang, Z.; Cui, Y. Membrane-free Zn/MnO_2 flow battery for large-scale energy storage. *Adv. Energy Mater.* **2020**, *10* (9), No. 1902085.

(7) Lei, J.; Jiang, L.; Lu, Y.-C. Emerging aqueous manganese-based batteries: Fundamental understanding, challenges, and opportunities. *Chem. Phys. Rev.* **2023**, *4* (2), No. 021307, DOI: 10.1063/5.0146094.

(8) Li, Y.; Zheng, X.; Carlson, E. Z.; Xiao, X.; Chi, X.; Cui, Y.; Greenburg, L. C.; Zhang, G.; Zhang, E.; Liu, C.; Yang, Y.; Kim, M. S.; Feng, G.; Zhang, P.; Su, H.; Guan, X.; Zhou, J.; Wu, Y.; Xue, Z.; Li, W.; Bajdich, M.; Cui, Y. In situ formation of liquid crystal interphase in electrolytes with soft templating effects for aqueous dual-electrode-free batteries. *Nat. Energy* **2024**, *9*, 1350−1359.

(9) Ye, X.; Han, D.; Jiang, G.; Cui, C.; Guo, Y.; Wang, Y.; Zhang, Z.; Weng, Z.; Yang, Q. H. Unraveling the deposition/dissolution chemistry of MnO_2 for high-energy aqueous batteries. *Energy Environ. Sci.* **2023**, *16* (3), 1016−1023.

(10) Xiao, X.; Zhang, Z.; Wu, Y.; Xu, J.; Gao, X.; Xu, R.; Huang, W.; Ye, Y.; Oyakhire, S. T.; Zhang, P.; Chen, B.; Cevik, E.; Asiri, S. M.; Bozkurt, A.; Amine, K.; Cui, Y. Ultrahigh-Loading Manganese-Based Electrodes for Aqueous Batteries via Polymorph Tuning. *Adv. Mater.* **2023**, *35* (33), No. 2211555.

(11) Ren, Y.; Li, H.; Rao, Y.; Zhou, H.; Guo, S. Aqueous MnO_2/Mn^{2+} Electrochemistry in Batteries: Progress, Challenges and Perspectives. *Energy & Environ. Sci.* **2024**, *17*, 425−441.

(12) Wang, Q.; Zhou, W.; Zhang, Y.; Jin, H.; Li, X.; Zhang, T.; Wang, B.; Zhao, R.; Zhang, J.; Li, W.; Qiao, Y.; Jia, C.; Zhao, D.; Chao, D. Rescue of dead MnO_2 for stable electrolytic Zn−Mn redox-flow battery: a metric of mediated and catalytic kinetics. *Natl. Sci. Rev.* **2024**, *11* (8), No. nwae230.

(13) Chuai, M.; Yang, J.; Tan, R.; Liu, Z.; Yuan, Y.; Xu, Y.; Sun, J.; Wang, M.; Zheng, X.; Chen, N.; Chen, W. Theory-Driven Design of a Cationic Accelerator for High-Performance Electrolytic MnO_2−Zn Batteries. *Adv. Mater.* **2022**, *34* (33), 2203249.

(14) Lei, J.; Yao, Y.; Wang, Z.; Lu, Y.-C. Towards high-areal-capacity aqueous zinc−manganese batteries: promoting MnO_2 dissolution by redox mediators. *Energy & Environ. Sci.* **2021**, *14* (8), 4418−4426.

(15) Chao, D.; Ye, C.; Xie, F.; Zhou, W.; Zhang, Q.; Gu, Q.; Davey, K.; Gu, L.; Qiao, S.-Z. Atomic engineering catalyzed MnO_2 electrolysis kinetics for a hybrid aqueous battery with high power and energy density. *Adv. Mater.* **2020**, *32* (25), 2001894.

(16) Zeng, X.; Liu, J.; Mao, J.; Hao, J.; Wang, Z.; Zhou, S.; Ling, C. D.; Guo, Z. Toward a reversible Mn^{4+}/Mn^{2+} redox reaction and dendrite-free Zn anode in near-neutral aqueous Zn/MnO_2 batteries via salt anion chemistry. *Adv. Energy Mater.* **2020**, *10* (32), 1904163.

(17) Möller, S.; Barwe, S.; Masa, J.; Wintrich, D.; Seisel, S.; Baltruschat, H.; Schuhmann, W. Online monitoring of electrochemical carbon corrosion in alkaline electrolytes by differential electrochemical mass spectrometry. *Angew. Chem.* **2020**, *59* (4), 1585−1589.

(18) Macauley, N.; Papadias, D. D.; Fairweather, J.; Spernjak, D.; Langlois, D.; Ahluwalia, R.; More, K. L.; Mukundan, R.; Borup, R. L. Carbon corrosion in PEM fuel cells and the development of accelerated stress tests. *J. Electrochem. Soc.* **2018**, *165* (6), F3148−F3160.

(19) Lim, K. H.; Oh, H. S.; Jang, S. E.; Ko, Y. J.; Kim, H. J.; Kim, H. Effect of operating conditions on carbon corrosion in polymer electrolyte membrane fuel cells. *J. Power Sources* **2009**, *193* (2), 575−579.

(20) Strandberg, L.; Shokhen, V.; Skoglundh, M.; Wickman, B. Carbon support corrosion in PEMFCs followed by identical location electron microscopy. *ACS Catal.* **2024**, *14*, 8494−8504.

(21) Zeng, H.; Zheng, Q.; Li, G.; Deng, J.; Jiang, Y.; Huang, R.; Liao, H. G.; Sun, S. G. Investigation of carbon corrosion in acidic media through in situ TEM and FTIR. *J. Phys. Chem. C* **2024**, *128* (35), 14683−14691.

(22) Varcoe, J. R.; Atanassov, P.; Dekel, D. R.; Herring, A. M.; Hickner, M. A.; Kohl, P. A.; Kucernak, A. R.; Mustain, W. E.; Nijmeijer, K.; Scott, K.; Xu, T.; Zhuang, L. Anion-exchange membranes in electrochemical energy systems. *Energy Environ. Sci.* **2014**, *7* (10), 3135−3191.

(23) Chao, D.; Zhou, W.; Ye, C.; Zhang, Q.; Chen, Y.; Gu, L.; Davey, K.; Qiao, S.-Z. An electrolytic Zn−MnO_2 battery for high-voltage and scalable energy storage. *Angew. Chem.* **2019**, *131* (23), 7905−7910.

(24) Wang, M.; Zheng, X.; Zhang, X.; Chao, D.; Qiao, S.-Z.; Alshareef, H. N.; Cui, Y.; Chen, W. Opportunities of aqueous manganese-based batteries with deposition and stripping chemistry. *Adv. Energy Mater.* **2021**, *11* (5), 2002904.

(25) Wolf-Gladrow, D. A.; Zeebe, R. E.; Klaas, C.; Körtzinger, A.; Dickson, A. G. Total alkalinity: The explicit conservative expression and its application to biogeochemical processes. *Mar. Chem.* **2007**, *106* (1−2), 287−300.

(26) Ferrell, J. R.; Rasmussen, M.; McNeary, W. W. Carbon Corrosion in Low-Temperature CO_2 Electrolysis Systems. *Sustain. Energy Fuels* **2024**, *8*, 3266−3278.

(27) Nourani, M.; Zackin, B. I.; Sabarirajan, D. C.; Taspinar, R.; Artyushkova, K.; Liu, F.; Zenyuk, I. V.; Agar, E. Impact of corrosion conditions on carbon paper electrode morphology and the performance of a vanadium redox flow battery. *J. Electrochem. Soc.* **2019**, *166* (2), A353.

(28) Derr, I.; Bruns, M.; Langner, J.; Fetyan, A.; Melke, J.; Roth, C. Degradation of all-vanadium redox flow batteries (VRFB) investigated by electrochemical impedance and X-ray photoelectron spectroscopy: Part 2 electrochemical degradation. *J. Power Sources* **2016**, *325*, 351−359.
(29) Oh, H. S.; Lim, K. H.; Roh, B.; Hwang, I.; Kim, H. Corrosion resistance and sintering effect of carbon supports in polymer electrolyte membrane fuel cells. *Electrochim. Acta* **2009**, *54* (26), 6515−6521.
(30) Jung, G. B.; Chuang, K. Y.; Jao, T. C.; Yeh, C. C.; Lin, C. Y. Study of high voltage applied to the membrane electrode assemblies of proton exchange membrane fuel cells as an accelerated degradation technique. *Appl. Energy* **2012**, *100*, 81−86.

https://doi.org/10.1021/acs.nanolett.5c02166
Nano Lett. 2025, 25, 10834−10839